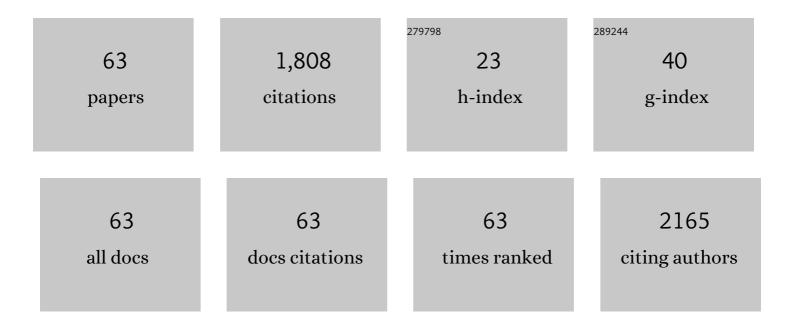
Liyun Cao

List of Publications by Year in descending order

Source: https://exaly.com/author-pdf/8401077/publications.pdf Version: 2024-02-01



#	Article	IF	CITATIONS
1	Tuning the coupling interface of ultrathin Ni ₃ S ₂ @NiV-LDH heterogeneous nanosheet electrocatalysts for improved overall water splitting. Nanoscale, 2019, 11, 8855-8863.	5.6	133
2	High Pseudocapacitance in FeOOH/rGO Composites with Superior Performance for High Rate Anode in Li-Ion Battery. ACS Applied Materials & Interfaces, 2016, 8, 35253-35263.	8.0	119
3	Adjusting the Chemical Bonding of SnO ₂ @CNT Composite for Enhanced Conversion Reaction Kinetics. Small, 2017, 13, 1700656.	10.0	111
4	Formation of hierarchical Ni3S2 nanohorn arrays driven by in-situ generation of VS4 nanocrystals for boosting alkaline water splitting. Applied Catalysis B: Environmental, 2019, 257, 117911.	20.2	92
5	Rape seed shuck derived-lamellar hard carbon as anodes for sodium-ion batteries. Journal of Alloys and Compounds, 2017, 695, 632-637.	5.5	71
6	In-situ optimizing the valence configuration of vanadium sites in NiV-LDH nanosheet arrays for enhanced hydrogen evolution reaction. Journal of Energy Chemistry, 2020, 47, 263-271.	12.9	66
7	V-Doping Triggered Formation and Structural Evolution of Dendritic Ni ₃ S ₂ @NiO Core–Shell Nanoarrays for Accelerating Alkaline Water Splitting. ACS Sustainable Chemistry and Engineering, 2020, 8, 6222-6233.	6.7	66
8	Improved Na Storage Performance with the Involvement of Nitrogen-Doped Conductive Carbon into WS ₂ Nanosheets. ACS Applied Materials & Interfaces, 2016, 8, 23899-23908.	8.0	65
9	Well-dispersed ultrasmall VC nanoparticles embedded in N-doped carbon nanotubes as highly efficient electrocatalysts for hydrogen evolution reaction. Nanoscale, 2018, 10, 14272-14279.	5.6	58
10	Controlling the Sn–C bonds content in SnO ₂ @CNTs composite to form <i>in situ</i> pulverized structure for enhanced electrochemical kinetics. Nanoscale, 2017, 9, 18681-18689.	5.6	56
11	Nanoporous NiAl-LDH nanosheet arrays with optimized Ni active sites for efficient electrocatalytic alkaline water splitting. Sustainable Energy and Fuels, 2020, 4, 2850-2858.	4.9	56
12	In situ synthesis of mesoporous C-doped TiO 2 single crystal with oxygen vacancy and its enhanced sunlight photocatalytic properties. Dyes and Pigments, 2017, 144, 203-211.	3.7	55
13	SnSe/r-GO Composite with Enhanced Pseudocapacitance as a High-Performance Anode for Li-Ion Batteries. ACS Sustainable Chemistry and Engineering, 2019, 7, 8637-8646.	6.7	55
14	Co,N-Codoped porous vanadium nitride nanoplates as superior bifunctional electrocatalysts for hydrogen evolution and oxygen reduction reactions. Nanoscale, 2019, 11, 11542-11549.	5.6	53
15	Cu/Cu2O@Ppy nanowires as a long-life and high-capacity anode for lithium ion battery. Chemical Engineering Journal, 2020, 391, 123597.	12.7	50
16	3D self-assembled VS ₄ microspheres with high pseudocapacitance as highly efficient anodes for Na-ion batteries. Nanoscale, 2018, 10, 21671-21680.	5.6	47
17	Realizing Fast Charge Diffusion in Oriented Iron Carbodiimide Structure for High-Rate Sodium-Ion Storage Performance. ACS Nano, 2021, 15, 6410-6419.	14.6	41
18	Rational Design of Vanadium-Modulated Ni ₃ Se ₂ Nanorod@Nanosheet Arrays as a Bifunctional Electrocatalyst for Overall Water Splitting. ACS Sustainable Chemistry and Engineering, 2021, 9, 12005-12016.	6.7	38

LIYUN CAO

#	Article	IF	CITATIONS
19	Controlling the layered structure of WS2 nanosheets to promote Na+ insertion with enhanced Na-ion storage performance. Electrochimica Acta, 2016, 222, 1724-1732.	5.2	28
20	Rice crust-like Fe3O4@C/rGO with improved extrinsic pseudocapacitance for high-rate and long-life Li-ion anodes. Journal of Alloys and Compounds, 2019, 804, 57-64.	5.5	27
21	N-doped TiO2/rGO hybrids as superior Li-ion battery anodes with enhanced Li-ions storage capacity. Journal of Alloys and Compounds, 2019, 784, 165-172.	5.5	27
22	Methanol-assisted synthesis of Ni ³⁺ -doped ultrathin NiZn-LDH nanomeshes for boosted alkaline water splitting. Dalton Transactions, 2020, 49, 1325-1333.	3.3	27
23	Enhanced cyclic performance of Cu2V2O7/ reduced Graphene Oxide mesoporous microspheres assembled by nanoparticles as anode for Li-ion battery. Journal of Alloys and Compounds, 2017, 724, 421-426.	5.5	25
24	Controllable Conversion from Single-Crystal Nanorods to Polycrystalline Nanosheets of NiCoV-LTH for Oxygen Evolution Reaction at Large Current Density. ACS Sustainable Chemistry and Engineering, 2020, 8, 16091-16096.	6.7	25
25	Ultrafine VN nanoparticles confined in Co@N-doped carbon nanotubes for boosted hydrogen evolution reaction. Journal of Alloys and Compounds, 2021, 853, 157257.	5.5	22
26	Heterostructured VN/Mo ₂ C Nanoparticles as Highly Efficient pH-Universal Electrocatalysts toward the Hydrogen Evolution Reaction. ACS Sustainable Chemistry and Engineering, 2021, 9, 15202-15211.	6.7	22
27	Structure-controlled synthesis and electrochemical properties of NH4V3O8 as cathode material for Lithium ion batteries. Electrochimica Acta, 2016, 212, 217-224.	5.2	20
28	Improved Li-Storage Properties of Cu ₂ V ₂ O ₇ Microflower by Constructing an in Situ CuO Coating. ACS Sustainable Chemistry and Engineering, 2019, 7, 6267-6274.	6.7	20
29	Tuning the morphologic and electronic structures of self-assembled NiSe/Ni3Se2 heterostructures with vanadium doping toward efficient electrocatalytic hydrogen production. Applied Surface Science, 2021, 542, 148598.	6.1	20
30	In Situ Construction of "Anchorâ€Like―Structures in FeNCN for Long Cyclic Life in Sodiumâ€Ion Batteries. Advanced Functional Materials, 2020, 30, 2000208.	14.9	19
31	Controlled WS2 crystallinity effectively dominating sodium storage performance. Journal of Energy Chemistry, 2020, 51, 143-153.	12.9	17
32	Exposing WS2 nanosheets edge by supports carbon structure: Guiding Na+ intercalation along (0 0 2) plane for enhanced reaction kinetics and stability. Chemical Engineering Journal, 2021, 411, 128554.	12.7	17
33	Dual modulation of morphology and electronic structures of VN@C electrocatalyst by W doping for boosting hydrogen evolution reaction. Chinese Chemical Letters, 2022, 33, 4781-4785.	9.0	17
34	Sulfur-regulated the binding configurations of nitrogen in three-dimensional graphene to improve lithium storage kinetics. Journal of Alloys and Compounds, 2019, 786, 1013-1020.	5.5	16
35	Vanadium-doped hierarchical Cu2S nanowall arrays assembled by nanowires on copper foam as an efficient electrocatalyst for hydrogen evolution reaction. Scripta Materialia, 2021, 196, 113756.	5.2	16
36	Design of dual-carbon modified MnO electrode improves adsorption and conversion reaction in Li-ion batteries. Ceramics International, 2018, 44, 3248-3254.	4.8	14

Liyun Cao

#	Article	IF	CITATIONS
37	Molybdenum and cobalt co-doped VC nanoparticles encapsulated in nanocarbon as efficient electrocatalysts for the hydrogen evolution reaction. Inorganic Chemistry Frontiers, 2022, 9, 870-878.	6.0	13
38	Synthesis, characterization and photocatalytic properties of nanoscale pyrochlore type Bi2Zr2O7. Materials Science and Engineering B: Solid-State Materials for Advanced Technology, 2019, 240, 133-139.	3.5	12
39	Carbon capsule confined Sb ₂ Se ₃ for fast Na ⁺ extraction in sodium-ion batteries. Sustainable Energy and Fuels, 2020, 4, 797-808.	4.9	12
40	Co–N-doped single-crystal V3S4 nanoparticles as pH-universal electrocatalysts for enhanced hydrogen evolution reaction. Electrochimica Acta, 2020, 335, 135696.	5.2	11
41	Vanadium -mediated ultrafine Co/Co ₉ S ₈ nanoparticles anchored on Co–N-doped porous carbon enable efficient hydrogen evolution and oxygen reduction reactions. Nanoscale, 2021, 13, 16277-16287.	5.6	11
42	Mo-Doped ultrafine VC nanoparticles confined in few-layer graphitic nanocarbon for improved electrocatalytic hydrogen evolution. Inorganic Chemistry Frontiers, 2020, 7, 4142-4149.	6.0	10
43	Guiding Fabrication of Continuous Carbon-Confined Sb ₂ Se ₃ Nanoparticle Structure for Durable Potassium-Storage Performance. ACS Applied Energy Materials, 2021, 4, 10391-10403.	5.1	10
44	Intrinsic defects promote rapid conversion of polysulfides on carbon surface to achieve high rate performance. Carbon, 2021, 183, 899-911.	10.3	10
45	High stability SEI film on the surface of Sb2O5/carbon cloth by coating SiO2 as high performance LIBs and SIBs anodes. Journal of Alloys and Compounds, 2022, 891, 162031.	5.5	10
46	Controlled Synthesis of V-Doped Heterogeneous Ni ₃ S ₂ /NiS Nanorod Arrays as Efficient Hydrogen Evolution Electrocatalysts. Langmuir, 2021, 37, 357-365.	3.5	10
47	Fe ₂ P encapsulated in carbon nanowalls decorated with well-dispersed Fe ₃ C nanodots for efficient hydrogen evolution and oxygen reduction reactions. Nanoscale, 2021, 13, 17920-17928.	5.6	10
48	Design of Cu2O coated Cu3V2O7(OH)2·2H2O microflower with in-situ crystallization process and enhanced Li-storage properties. Journal of Electroanalytical Chemistry, 2019, 835, 186-191.	3.8	9
49	Dual carbon composited with Co9S8 through C-S bond as a high performance Binder-Free anode for Sodium-Ion batteries. Applied Surface Science, 2022, 582, 152406.	6.1	9
50	A new approach to preparing Bi ₂ Zr ₂ O ₇ photocatalysts for dye degradation. Materials Research Express, 2018, 5, 015039.	1.6	8
51	Design of an ultra-stable Sb2Se3 anode with excellent Na storage performance. Journal of Alloys and Compounds, 2019, 810, 151930.	5.5	8
52	Self-templated induced carbon-supported hollow WS ₂ composite structure for high-performance sodium storage. Journal of Materials Chemistry A, 2021, 9, 21366-21378.	10.3	8
53	Layered-structure (NH ₄) ₂ Mo ₄ O ₁₃ @N-doped porous carbon composite as a superior anode for lithium-ion batteries. Chemical Communications, 2020, 56, 7757-7760.	4.1	7
54	Facile synthesis of reduced graphene oxide/NH ₄ V ₃ O ₈ with high capacity as a cathode material for lithium ion batteries. Micro and Nano Letters, 2017, 12, 940-943.	1.3	5

LIYUN CAO

#	Article	IF	CITATIONS
55	Inducing [100]-orientated plate-like α-MoO3 to achieve regularly exfoliated layer structure enhancing Li storage performance. Journal of Materials Science: Materials in Electronics, 2021, 32, 3006-3018.	2.2	5
56	<i>In situ</i> construction of superhydrophilic crystalline Ni ₃ S ₂ @amorphous VO _{<i>x</i>} heterostructure nanorod arrays for the hydrogen evolution reaction with industry-compatible current density. Dalton Transactions, 2022, 51, 7234-7240.	3.3	5
57	Controlling the thickness of amorphous layer on Cu3(PO4)2 particle for promoted sodium storage reversibility as a conversion-reaction-based cathode. Journal of Electroanalytical Chemistry, 2019, 852, 113406.	3.8	4
58	Polyethylene glycol (PEG)-assisted synthesis of self-assembled cactus-like NH4V3O8 for lithium ion battery cathode. Scripta Materialia, 2020, 183, 75-80.	5.2	4
59	A N/S-codoped disordered carbon with enlarged interlayer distance derived from cirsium setosum as high-performance anode for sodium ion batteries. Journal of Materials Science: Materials in Electronics, 2019, 30, 21323-21331.	2.2	2
60	Equal contents of intrinsic defects and oxygen-containing defects promote carbon electrodes to achieve high sulfur loads. Journal of Nanostructure in Chemistry, 0, , 1.	9.1	2
61	A thick titanium dioxide layer formed by Co-doping on a carbon surface promotes the polysulfide-adsorption ability in Li–S batteries. Sustainable Energy and Fuels, 2021, 5, 4153-4160.	4.9	1
62	Binding Molybdenum selenide with dual conductive carbon as Self-Supporting anode for an efficient sodium storage. Applied Surface Science, 2021, 570, 151122.	6.1	1
63	A three-dimensional coral-like Zn,O-codoped Ni3S2 electrocatalyst for efficient overall water splitting at a large current density. Sustainable Energy and Fuels, 2022, 6, 466-473.	4.9	О